ELECTRO-HYDRODYNAMIC MODELING OF ELECTROSPRAY IONIZATION: CAD FOR A μFLUIDIC DEVICE – MASS SPECTROMETER INTERFACE

Jun Zeng[(1)], Daniel Sobek[(2)] and Tom Korsmeyer[(1)]
(1) Coventor, Inc., 625 Mount Auburn Street, Cambridge, MA 02138
(2) Agilent Technologies, Inc., Agilent Laboratories, 3500 Deer Creek Road, Palo Alto, CA 94304
e-mail: jun.zeng@coventor.com

ABSTRACT

We report on full-dimensional, multi-phase, electro-hydrodynamic simulations of electrospray dynamics and our simulation method derived from Melcher & Taylor's leaky dielectric fluids model [1]. The method is first validated via the Melcher-Taylor apparatus and corresponding analytical solution, and then applied to understanding the formation of Taylor cones, a key issue in designing a μfluidic device with an integrated mass-spectrometer interface.
The simulation results show excellent agreement with the Melcher-Taylor solution. The transient full-dimensional simulation of Taylor cone formation shown here is believed the first published result of this kind.
Experiment results in electrospray dynamics are presented for qualitative comparison.

Keywords: leaky-dielectric fluid, electrohydrodynamics, microfluidics, electrospray ionization, simulation

INTRODUCTION

During the last decade, various mass spectrometric (MS) techniques have been introduced for the analysis of biopolymers such as peptides, proteins, oligonucleotides, and oligosaccharides. Such applications require the utmost spectrometric sensitivity and thus have excited much research activity. An improvement in sensitivity can be achieved by integrating an on-chip chromatographic separation system and by improvements of the chip-MS interface [2][4]. A miniaturized fluidic analysis apparatus, or a micro total analysis system (μTAS), offers the unique advantages of increased sample throughput, better reproducibility, higher sensitivity, and significantly lower cost per analysis over conventional, higher flow-rate analyses [3]. As a perfect source of large charge-to-mass ions of large bio-molecules, and one of the most versatile continuous-flow ionization techniques, electrospray ionization (ESI) is being investigated as the means to couple μTAS and MS to achieve sensitive and selective detection of analytes for qualitative and quantitative analysis [3][4].
ESI generates gas phase ions from solutes in liquid solutions. Figure 1 illustrates an on-chip μESI interface. The liquid sample from the μfluidic device is fed into the ESI tip. Coupling between electrostatic forces and multiphase hydrodynamics results in the formation of a capillary jet with a cone-shaped base, which narrows down to a fine liquid filament. Together, these comprise the so-called Taylor cone. Interfacial instabilities break this filament into charged droplets, which subsequently experience Coulombic explosions and evaporation, turning into a cloud of gas-phase ions representative of the species contained in solution. The gas-phase ions flow into an MS device for further analysis. The formation of the Taylor cone is the topic of this paper [5].
Much of the published research on ESI has been focused on experiments and theoretical analyses (for a review see [6]). Numerical tools were used to find a steady-state Taylor cone shape by solving reduced-order equations with simplifications based on experimental observation (e.g., [7]). In this paper, we are reporting, for the first time, a transient, full-dimensional simulation of Taylor cone formation, based on the Navier-Stokes equation and the Melcher-Taylor leaky dielectric model.
In the next section, we summarize the modeling approach. Following that, validation cases are presented, with comparisons to the analytical solution of Melcher-Taylor. Then we show example applications of the simulation as would be used in ESI interface design. Experiments have been conducted to guide simulations. A brief description of the experiment setup and results are presented before a concluding section.

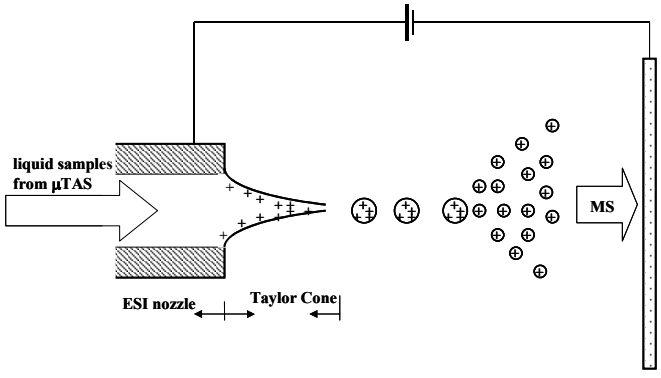

Fig. 1: Schematic of an ESI interface between a μfluidic unit and an MS.

MODELING APPROACH

Leaky Dielectric Fluids. The principles for dealing with electrified fluids were summarized by Melcher and Taylor [1] (for a recent review see [8]). It was discovered that it is impossible to account for most of the electrical phenomena involving moving fluids given the assumption that the fluid

is either a perfect dielectric or a perfect conductor, because both the permittivity and the conductivity affect the flow.

An electrified liquid always contains free charge. Although the charge density may be small enough to ignore bulk conduction effects, the charge will accumulate at the interfaces between fluids. The presence of this interfacial charge will result in an additional interfacial stress, especially a tangential stress, which in turn will modify the fluid dynamics.

Electrostatic Field. The assumption of electro-quasistatics is contained in electrohydrodynamics (EHD). Two phases of fluids are involved in the current study: the gas phase (e.g., air) acts as an insulator and the liquid phase (e.g., aqueous solution) acts as a leaky dielectric.

As noted above, if the bulk free charge density in the liquid is assumed to be zero, then the electric potential ϕ is irrotational and divergence-free throughout the field. The presence of the interfacial charge density S creates an electric field discontinuity in the direction normal to the interface. The accumulation rate of this interfacial charge density S is described by the continuity condition for conservation of charge expressed via Ohm's law.

To summarize, the governing equation of the electrostatic field is

$$\nabla^2 \phi = 0 \qquad (1)$$

in the bulk liquid and the air. At the interfacial boundary,

$$\vec{n} \cdot (\varepsilon_l \nabla \phi_l - \varepsilon_g \nabla \phi_g) = S \qquad (2)$$

where $\vec{n}$ is the unit normal of the interface pointing into the air, ε is the dielectric constant, subscript g indicates the gas phase, and subscript l indicates the liquid phase. The interfacial charge density S is

$$\frac{dS}{dt} = -\vec{n} \cdot \sigma \nabla \phi_l \qquad (3)$$

where d/dt is the Lagrangian derivative, and σ is the conductivity of the liquid. Equation (3) describes the process of interfacial charge accumulation.

Electrohydrodynamic Forces. An electrostatic field exerts additional mechanical forces on liquids. Such an electromechanical force density can be derived from thermodynamics assuming a closed system [9],

$$\vec{F}^{EM} = \rho_e \vec{E} - \frac{1}{2} |\vec{E}|^2 \nabla \varepsilon + \nabla [\frac{1}{2} (\varepsilon - \varepsilon_0) |\vec{E}|^2] \qquad (4)$$

where ρ_e is the net free charge density, and $\vec{E} = -\nabla \phi$.

To interpret equation (4), one may observe that the first two terms comprise the broadly accepted Korteweg-Helmholtz (K-H) electromechanical force density: that due to free net charge and that due to polarization [1]. In order to understand the origin of the third term, one needs to examine the Maxwell electromechanical stress tensor that the K-H expression is derived from.

Under the framework of the Maxwell electromechanical stress tensor, the pressure, which is the negative mean normal stress, has an electromechanical component in addition to the hydrodynamic component. In other words, to build up a fully-coupled EHD formulation under the Maxwell stress tensor framework, in addition to adding a source term (the K-H force density) to the momentum equation; apparently, one must also modify the pressure boundary conditions to incorporate the electromechanical pressure component.

However, Equation (4) offers an alternative approach. It includes the gradient of the electromechanical pressure as an additional component of the electromechanical force density, preserving the pressure itself as purely hydrodynamic.

The leaky-dielectric fluid code used for the simulations here is based on a well-established multi-phase flows hydrodynamics code [10]. Implementation of equation (4) has the advantage that it minimizes the modification needed by isolating all of the electromechanical effects on the hydrodynamics as an additional body force density. The EHD coupling is achieved via an additional source term in the momentum equation alone, eliminating the necessity to modify the existing pressure-related boundary conditions.

From a physical perspective, the third term in equation (4) represents the component of the electromechanical force density due to the non-uniformity of the electric field.

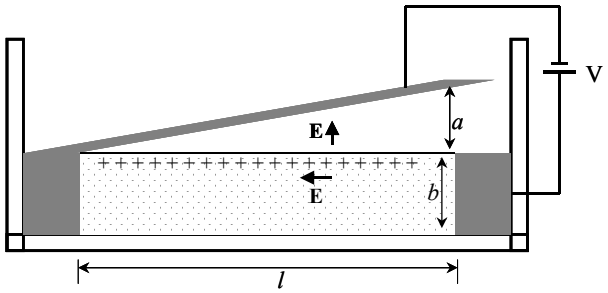

Fig. 2: Melcher-Taylor apparatus. The induced interfacial charge acts in concert with the electric field resulting in a counterclockwise cellular convection.

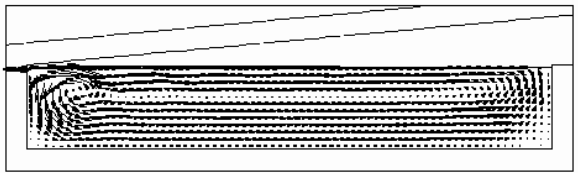

Fig. 3: Velocity plot (simulation). The density, viscosity, conductivity and relative permittivity of the liquid are *900 Kg/m^3, 0.055 Kg/m/s, 8.05e-6 S/m* and *3, respectively*. The voltage is *10KV*. *a=0.022 m, b=0.038m,* and *l=0.24m*. Time frame shown is *t=5.5s* (steady state).

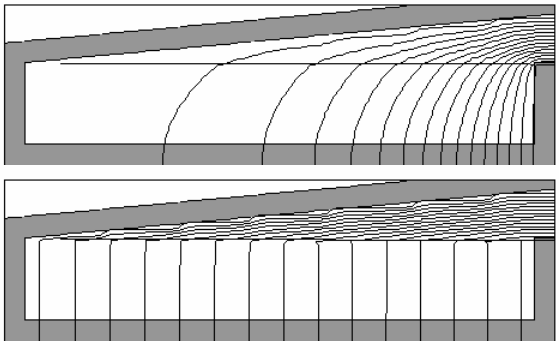

Fig. 4: Steady-state iso-potential contours (simulation). Above: liquid is a perfect dielectric. Below: liquid is a leaky dielectric.

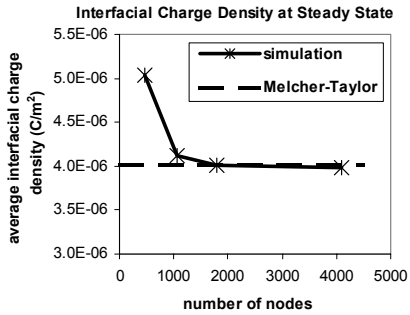

Fig. 5: Steady-state average interfacial charge density plotted versus mesh resolution. The dashed line is the Melcher-Taylor steady-state solution.

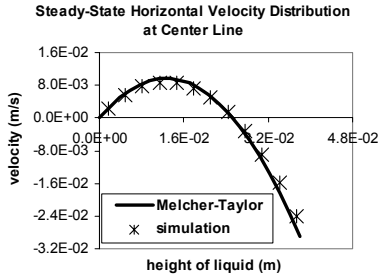

Fig. 6: The steady-state horizontal velocity distribution along the centerline. 1794 nodes are used.

VALIDATION – MELCHER-TAYLOR APPARATUS

Figure 2 illustrates the Melcher-Taylor apparatus [1]. A shallow, slightly conducting liquid fills an insulating container to depth *b*. An electrode (at left) extends over the interface, is canted, and reaches a height *a* at the extreme right. The length *l* is much larger than *a* and *b*. The discontinuity of the electric field at the interface results in a non-zero interfacial charge density, which together with the electric field in the liquid (pointing to the left) induces an electric shear force on the interface. This shear force generates a counter-clockwise cellular convection. Figure 3 shows a simulation of the electrified circulatory flow. Figure 4 shows how the electric potential distribution is greatly modified when the modeling of the liquid is switched from an insulator to a leaky dielectric. A discontinuity of the electric field now occurs at the interface, due to the presence of the interfacial charge.

Figure 5 shows a mesh convergence study: the average interfacial surface charge density at steady state as a function of mesh resolution. A good convergence behavior is observed. To test the accuracy of the coupling between the electromechanical forces and the hydrodynamics, the steady-state horizontal velocity profile is plotted in Figure 6. The agreement between the simulation and the Melcher-Taylor solution is excellent.

ESI SIMULATION: IMPACT OF FLOW RATE

Figure 1 illustrated the ESI apparatus modeled in our simulations. A constant electric potential difference V_0 is maintained between the conducting cylindrical needle and the metal plate, which is separated by a distance *L*. The radius of the needle orifice is R_0. A semi-insulating liquid of density ρ, viscosity μ, electric conductivity κ and permittivity ε flows through the needle with a constant volumetric flow rate *Q*. The surface tension coefficient between the liquid and air is γ. The permittivity of vacuum is ε_0. Formation of the Taylor cone can be quantified by the electrical current *I* through the jet, the jet radius *R*, and the

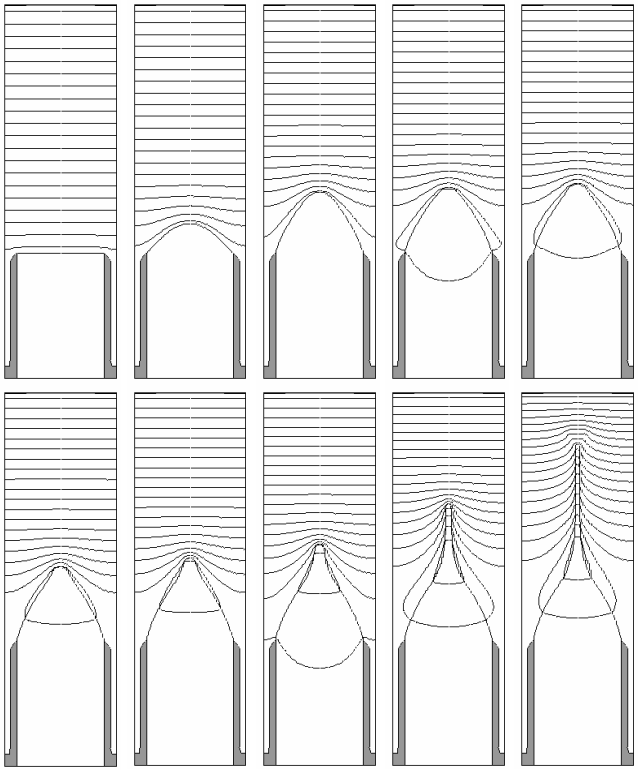

Fig. 7: Transient formation of a Taylor cone (simulation). The flow rate is 1423. The normalized times for the first three pictures are 0, 1022 and 2045; the following pictures are 68 apart. The Taylor cone shape (outlined by the curves originated from the tip of the nozzle) is plotted together with iso-potential lines.

cone shape.

A group of parameters are introduced to non-dimensionalize the problem [11]: $Q_0 = \gamma\varepsilon_0/(\rho\kappa)$; $t_0 = \varepsilon/\kappa$; $I_0 = \gamma\sqrt{\varepsilon_0/\rho}$ and $d_0 = \sqrt[3]{\gamma\varepsilon_0{}^2/(\pi^2\rho\kappa^2)}$ with respect to the volumetric flow rate, time, electric current and jet radius. Data reported hereafter are dimensionless.

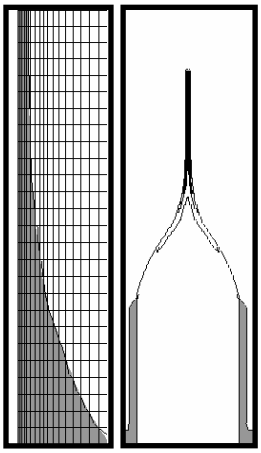

Figure 8: A developed Taylor cone. Left: a close-up view of the jet with the mesh superimposed on it to show good resolution. Right: the shape of the Taylor cone plotted together with the contour lines of the charge density distribution.

The detailed shape of the nozzle determines the surrounding electric field and therefore affects the formation of the Taylor cone significantly, as experienced in simulations and also reported by experiments [7]. Figure 7 shows a successful generation of a Taylor cone. The Taylor cone shape (curves originating at the tip of the nozzle) is plotted together with iso-potential lines indicating the evolution of the surrounding electric field. Figure 8 shows a fully developed Taylor cone plotted with the contour lines of the charge density distribution. The figure shows that the free

charge is concentrated in the jet region; there is a non-zero charge distribution on the cone surface; and there is no

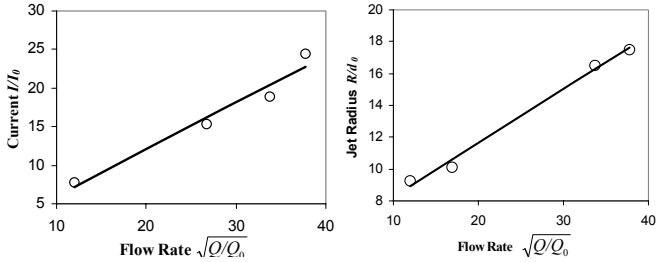

Fig. 9: Taylor cone radius and current as function of flow rate (simulation).

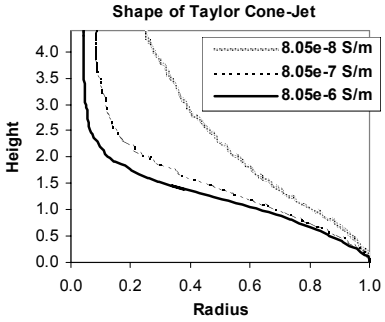

Fig. 10: Shape of the Taylor cone as a function of liquid electric conductivity (simulation).

charge inside the bulk liquid assumed in the leaky dielectric model. The mesh at the jetting region is also shown indicating good resolution there.

For a given capillary and liquid, the flow rate Q is one of the key operation parameters. Figure 9 shows the variation of the electric current I and the jet radius R with respect to flow rate Q, obtained via simulation. It is observed that $I / I_0 \propto \sqrt{Q / Q_0}$ and $R / d_0 \propto \sqrt{Q / Q_0}$, as has been reported in experiments [11].

The electric properties of the liquid also have an impact on the shape of the Taylor cone. Figure 10 shows a comparison of the Taylor cone shape for different electric conductivities.

ESI EXPERIMENTS

A custom ESI testing station has been setup on the stage of a microscope (Nikon Eclipse TE300) with a 14-bit high frame-rate CCD camera (Pluto CCD, PixelVision) mounted at its side-port. A syringe pump (Harvard Apparatus, model 22) and a 25-4000 nanoliter per minute flow sensor (engineering sample from Upchurch Scientific) are used to control liquid feed. An electric field is established between a grounded metal-coated capillary tip and a stainless steel counter electrode via a 2.5 kV power supply (Stanford Scientific, model PS325). The distance between the tip and counter electrode is adjusted using a micrometer head. A 400 MHz bandwidth transimpedance amplifier (Femto GMbH, model DLPCA-200) is employed to measure the ESI current emitted from the tip. Experiment results are shown in figure 11. Left shows an electrospray plume generated using the electrospray chip described in [4]. Right shows a close-up view of the Taylor cone. The experiment image qualitatively agrees with the simulation results of Figure 8.

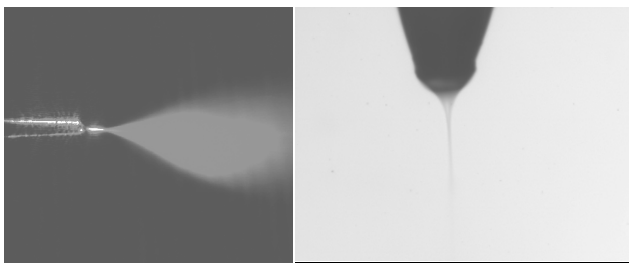

Fig. 11: Experiment images. Left is a micrograph showing an electrospray emitted from a gold-coated *60 μm* diameter kapton tip. Right shows a Taylor cone that is formed at a capillary tip of diameter *32 μm*. V_0*=1600 V*, tip-to-counter-electrode distance is *1.5 mm*. The liquid is 1:1 acetonitrile:H2O (v/v), of conductivity *0.012 S/m*. The volumetric flow rate is *5 nanoliter per second*.

CONCLUSIONS

We have presented a numerical methodology for investigating electrospray dynamics, based on Melcher and Taylor's leaky-dielectric liquid theory. Numerical results have been validated against analytical solutions and the agreement is excellent.

Simulations studying the formation of the Taylor cone have identified the key issues in designing a μfluidic interface between a μTAS and MS. These studies show that the feeding flow rate and the electric conductivity of the liquid affect the behavior of the Taylor cone in agreement with published experimental observation.

Experiments on electrospray dynamics have been conducted and are used as a guide for the simulations.

The simulation of the formation of a Taylor cone reported here is believed to be the first published results of this kind.

Acknowledgment

Zeng and Korsmeyer acknowledge the support of The Defense Advanced Research Projects Agency (DARPA) under contract DAAD10-00-1-0515 from the Army Research Office to the University of Texas M.D. Anderson Cancer Center. Zeng would like to thank Dr. C. W. Hirt for helpful discussions.

References

[1] J. R. Melcher and G. I. Taylor, ""Electrohydrodynamics: a review of the role of interfacial shear stresses", Annu. Rev. of Fluid Mech., 1, 1969, pp. 111–146.

[2] H. D. Meiring, et al., "Nanoscale LC-MS: technical design and applications to peptide and protein analysis", J. Sep. Sci., 25, 2002, pp.557-568

[3] G. A. Schultz, et al., "A fully integrated monolithic microchip electrospray device for mass spectrometry", Analytical Chemistry, Vol. 72, No. 17, 2000, pp. 4058-4063

[4] K. Killeen et al., "Chip-MS: a polymeric microfluidic device with integrated mass-spectrometer interface", Micro Total Analysis Systems 2001, 2001, pp.331-332

[5] R. Juraschek, F. W. Rollgen, "Pulsation phenomena during electrospray ionization", Inter. J. of Mass Spec., 177, 1998, pp.1-15

[6] A. M. Ganan-Calvo, "On the theory of electrohydrodynamically driven capillary jets", J. Fluid Mech., Vol. 335, 1997, pp. 165-188

[7] M. M. Hohman, et al., "Electrospining and electrically forced jets. II. Applications", Phys. Fluids, Vol. 13, No. 8, 2001, pp. 2221-2236

[8] D. A. Saville, "Electrohydrodynamics: The Taylor-Melcher leaky-dielectric model," Annu. Rev. Fluid Mech., 29, 1997, pp. 27-64

[9] J. R. Melcher, "Continuum Electromechanics", The MIT Press, 1981

[10] C. W. Hirt and B. D. Nichols, "Volume of Fluid (VOF) Method for the Dynamics of Free Boundaries", Journal of Computational Physics, Vol. 39, 1981, pp. 201-225

[11] A. M. Ganan-Calvo, “The Surface Charge in Electrospraying: its Nature and its Universal Scaling Laws”, J. Aerosol. Sci., Vol. 30, No. 7, 1999, pp. 863-872